D. Arnal°, J. Reneaux▷ & G. Casalis°

Numerical and Experimental Studies Related to Skin Friction Drag Reduction Problems

Abstract

This paper gives an overview of some recent investigations conducted at ONERA in order to improve the techniques for laminar flow control. The first part deals with the problem of leading edge contamination. It is shown that suction and the Gaster bump can significantly increase the Reynolds number at which contamination occurs. The second part of the paper is devoted to applications of numerical tools aimed at predicting the onset of transition.

Introduction

Among the different techniques which could be applied to reduce the drag of transport aircraft, laminar flow technology seems to have the greatest potential. The importance of the problem and the associated economic gains are highlighted by the large number of studies currently being carried out in the United States and in Europe. In France, ONERA is deeply involved in several national and European programmes (Falcon 900, A 320 fin, ELFIN project). Besides practical results directly applicable to free flight conditions, these numerical and experimental studies gave the opportunity to obtain fundamental information concerning the transition problem. The objective of this paper is to give a survey of these results, by showing how such studies have improved our knowledge of the transition mechanisms and our capability to model them.

For swept wings, a substantial region of laminar flow can be maintained by controlling the development of crossflow and/or Tollmien-Schlichting (TS) disturbances. This control can be carried out either by adequately shaping the wing (NLF: Natural Laminar Flow) or by applying suction at the wall (LFC: Laminar Flow Control). Given the typical leading edge sweep angles and chord Reynolds numbers of transport aircraft wings, most of the research effort is devoted to the combination of these techniques (HLFC: Hybrid Laminar Flow Control). However, it is first necessary to ensure that the attachment line boundary layer is laminar, i.e. to avoid the problems of leading edge contamination. This phenomenon, by which the turbulence of the fuselage boundary layer is convected along a swept leading edge, is likely to occur on transport aircraft causing the wing boundary layer to become fully turbulent. A survey of these problems can be found in the AGARD Report (1992).

The first part of this paper presents results obtained during wind tunnel tests for two anti-contamination devices, namely a Gaster bump and a porous leading

edge allowing to apply suction along the attachment line. The second part of the paper is devoted to the development of numerical methods aimed at predicting the transition location as accurately as possible. These methods are applied for several problems where different stabilization techniques are tested.

Leading edge contamination problems

It is well known that leading edge contamination occurs on a swept wing as soon as a leading edge Reynolds number $\bar{R}$ exceeds a critical value close to 250, see Pfenninger (1965) and Poll (1978). $\bar{R}$ is defined as:

$$\bar{R} = \frac{W_e \eta}{\nu_e}, \quad \text{with} \quad \eta = \sqrt{\frac{\nu_e}{k}},$$

where ν_e is the kinematic viscosity, W_e is the mean flow component parallel to the attachment line and K is the velocity gradient along the surface and normal to the leading edge.

As typical values of $\bar{R}$ near the root are of the order of 800-1000 for large transport aircraft, it is necessary to develop specific tools to delay the onset of leading edge contamination. This is in fact the first problem to solve for maintaining laminar flow on a wing: if the attachment line flow is turbulent, the NLF, LFC or HLFC systems will become useless.

Gaster bump

A successful device to prevent leading edge contamination is the Gaster bump (Gaster, 1967). It consists of a small fairing which is placed on the leading edge close to the wing root. It is shaped in such a way that the contaminated turbulent boundary layer is brought to rest at a stagnation point on the upstream side whilst a "clean" laminar boundary layer is generated on the downstream side.

Several Gaster bumps were tested in a water channel and in the transonic T2 wind tunnel at CERT ONERA. These experiments allowed to optimize some geometrical parameters of the bumps, while numerical investigations gave some insight into the transition mechanisms.

An example of the results is presented in Fig. 1, which shows a comparison between the measured and computed transition lines around a bump tested in the T2 wind tunnel during the preparation of flight tests performed by Dassault Aviation. Due to the strong deflection of the flow on both sides of the device, a powerful crossflow instability is generated and transition takes place at a short distance from the attachment line. Further downstream (in the spanwise direction), the transition front moves up to larger chordwise distances. When $\bar{R}$ increases, transition around the bump occurs closer and closer to the attachment line. This could explain the efficiency limitation of this kind of device.

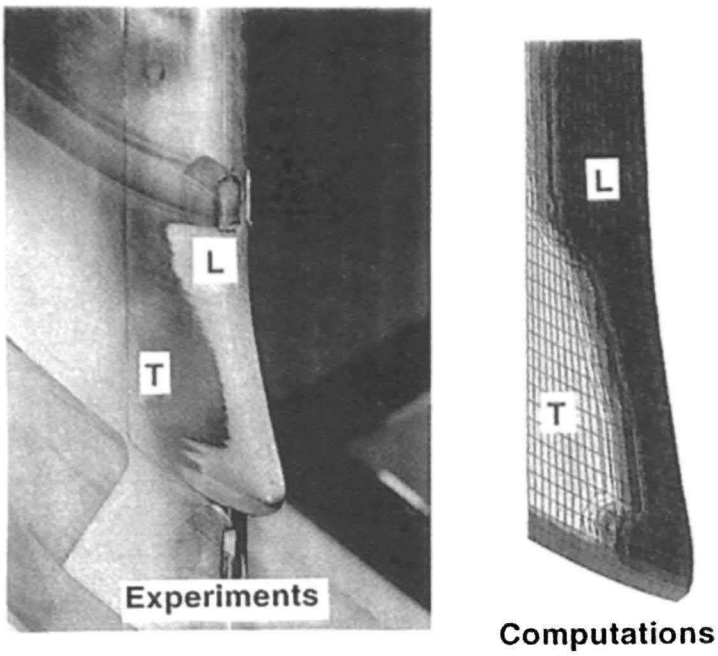

Figure 1: Transition front around a Gaster Bump, sweep angle $\varphi = 35°$, $M_\infty = 0.74$ (L: Laminar, T: Turbulent). Comparison between experiments (sublimation) and computations (transition criteria, Arnal *et al.*, 1995).

Suction (without or with Gaster bump)

The first results related to the effect of suction on contamination were obtained from DNS carried out by Spalart (1988). These computations showed that contamination can be delayed up to $\bar{R} \approx 350-400$ for $K = -1$. K is a dimensionless suction parameter:

$$K = \frac{V_w}{W_e}\bar{R}.$$

A first series of experiments carried out at CERT ONERA were performed on a small model by Juillen & Arnal (1995). With $K = -1.15$, contamination first appeared at $\bar{R} = 470$, but the small dimensions of the wind tunnel did not allow higher values of $\bar{R}$ to be investigated. Therefore ONERA decided to perform tests in the F2 wind tunnel at Le Fauga Mauzac in order to study this phenomenon at large values of $\bar{R}$. The chosen experimental support was a constant chord ($C = 1.2$ m) swept wing model generated from a symmetrical airfoil with a radius R of 0.2 m near the leading edge. The phenomenon of leading edge contamination was studied at sweep angles of 40° and 50° by fixing the model to the tunnel wall.

The objective of the tests was to delay leading edge contamination either by the use of a Gaster bump or by applying suction along the leading edge or

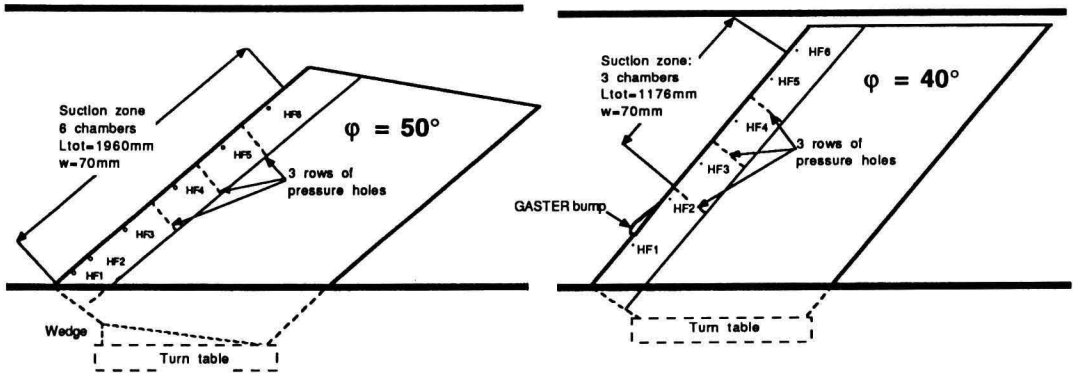

Figure 2: Experimental set-up without bump (left) and with bump (right). HF: hot films.

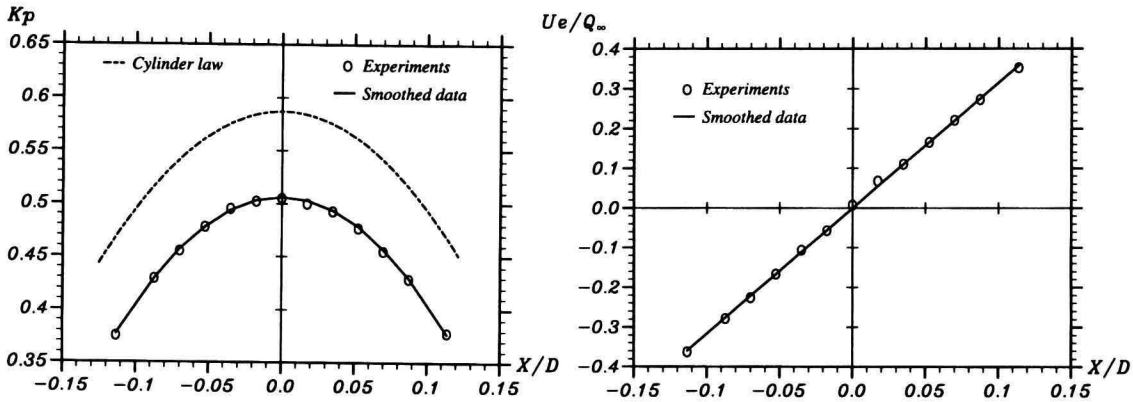

Figure 3: Experimental determination of the velocity gradient.

a combination of both. Fig. 2 shows the two leading edges which have been tested; the first one consists of six independent suction chambers fitted along the leading edge and the second one combines a Gaster bump with three leading edge suction chambers downstream of the bump. Three-dimensional computations were carried out to determine the effect of the wind tunnel walls on the pressure distributions and boundary layers of the configurations tested.

The chordwise width of the suction panel was about 70 mm, i.e. 35 mm on each side of the attachment line. The titanium perforated panel was laser drilled by AS&T company and the mean diameter of the holes was about 50 μm. The model instrumentation consisted of 3 rows of surface pressure taps aligned normal to the leading edge. Furthermore, 12 pressure taps were installed inside the suction chambers in order to evaluate the operation of the suction system. Leading edge contamination was detected by flush-mounted surface hot films. The position of the hot film is shown in Fig. 2.

The values of $\bar{R}$ were computed using pressure measurements made around

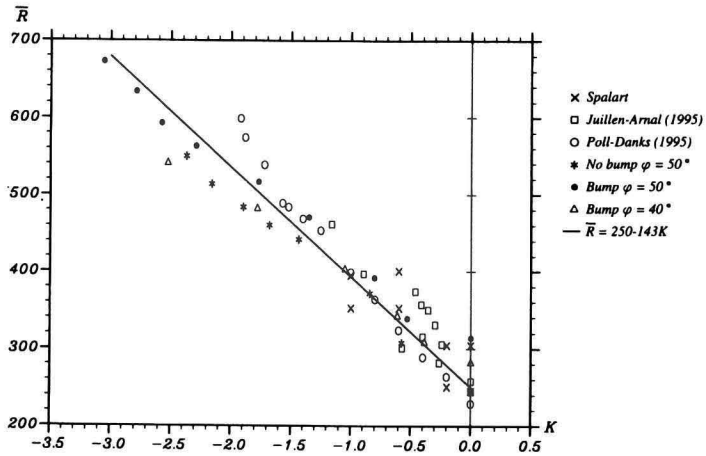

Figure 4: Leading edge contamination Reynolds numbers: summary of the results.

the leading edge. The computation of the velocity gradient K requires a precise analysis in order to be sure that small perturbations, caused for example by some defects in the geometry of the porous wall, do not introduce discrepancies into the computation. It was therefore decided to smooth the measured K_p distributions using second order polynomials (with $K_p = (P - P_\infty)/\frac{1}{2}\rho_\infty Q_\infty^2$, where P is the static pressure). Smoothing was carried out by the least square method in the interval $-0.2 < X/R < +0.2$. As an example, Fig. 3 shows the evolution of the measured pressure distribution and of the dimensionless normal velocity component U_e/Q_∞ as a function of X (curvilinear distance normal to the leading edge) for the case $Q_\infty = 60$ m/s and $\phi = 40^o$. After smoothing, K and $\bar{R}$ can be accurately determined. The final values of $\bar{R}$ differ by about 10% from those of the potential flow around a circular cylinder.

Fig. 4 shows the evolution of $\bar{R}$ corresponding to the onset of leading edge contamination (first spots) as a function of the suction parameter K. The results obtained without Gaster bump for $\phi = 50^o$ are compared with the DNS results by Spalart (1988) and with the experimental data currently available (Juillen & Arnal, 1995; Poll & Danks, 1995). Without suction, leading edge contamination occurs for $\bar{R} \approx 250$, as expected. Application of suction causes the onset of contamination to be delayed to $\bar{R} \approx 550$ for the maximum suction rate attainable in the experiments ($K = -2.4$).

For the configuration with a Gaster bump at $\phi = 50^o$, leading edge contamination in the absence of suction occurs at $\bar{R} = 320$, a value which is lower than that obtained in other previous experiments. As soon as the flow over the bump is fully turbulent, the data with and without bump become close together (within the experimental uncertainty). The porosity of the porous leading edge fitted with the bump was larger than that of the leading edge without bump, so that the dimensionless suction parameter could be increased up to $K = -3.07$. This

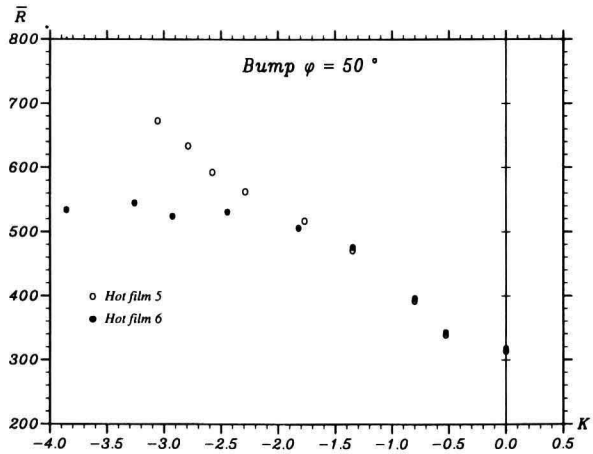

Figure 5: Leading edge contamination Reynolds numbers at two spanwise positions.

allowed to delay the onset of leading edge contamination up to $\bar{R} = 670$. The data for the onset of contamination without bump are fairly well represented by the following relationship:

$$\bar{R} = 250 - 143\ K.$$

The previous results were deduced from the time signals delivered by the hot films placed just before the end of the porous wall (hot film 6 without bump, hot film 5 with bump, see Fig. 2). The leading edge fitted with a bump was equipped with an additional sensor (hot film 6) after the end of the porous wall. Fig. 5 shows the leading edge contamination limits indicated by hot films 5 and 6 for the case with bump and $\phi = 50^o$. The signals delivered by hot film 6 indicate that downstream of the sucked region, transition cannot be delayed above $\bar{R} \approx 550$, which roughly corresponds to the lower limit of "natural transition" (see next paragraph).

Numerical approaches for "natural" transition

Assuming that leading edge contamination is avoided, transition will occur through the amplification of "natural" disturbances. This linear, local stability theory and the e^n method are widely used to analyse this type of transition process. The following examples illustrate the efficiency and the limitations of the classical prediction methods and show how it is possible to improve the accuracy of these methods. The first example (localized surface heating) shows that the "old" e^n method is still useful for parametric studies. The second example (effect of suction) demonstrates how more recent approaches make it possible to take into account nonlinear phenomena. In the third example (leading edge instability), it is shown that classical TS waves are not always the most relevant ones for linear stability problems.

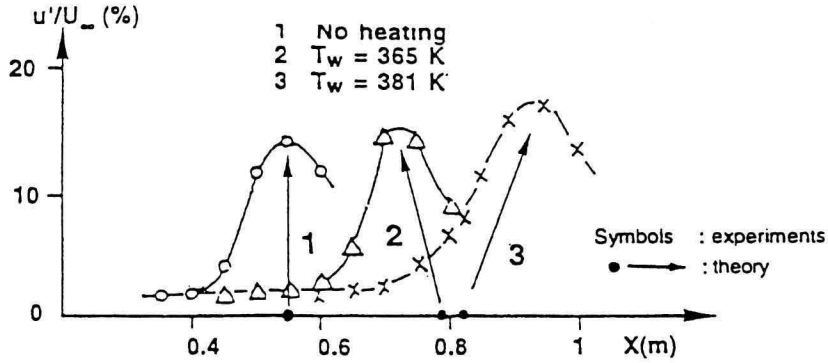

Figure 6: Effect of a localized surface heating on transition location.

Linear, local theory: application of the e^n method to the problem of localized heating

The shortcomings and limitations of the classical e^n method (based on local stability computations) are well known and have been discussed in several papers (e.g. Arnal, 1993; Arnal *et al.*, 1995). However, this method remains a very practical and efficient tool, especially for parametric studies. For a given test model and for a given disturbance environment, it is often able to predict the variation of the transition location when changing a parameter which governs the stability properties of the mean flow (pressure gradient, wall temperature, suction rate for instance).

To illustrate the usefulness of the e^n method for this kind of analysis, let us consider the problem of transition control by a localized surface heating (in air). The principle of this new stabilization technique is as follows. The wall is heated over a short streamwise distance, and a relaxation region develops downstream of the strip. In this region, the boundary layer temperature close to the wall is larger than the wall temperature, so that the boundary layer "sees" a cold wall. According to the linear stability theory, this leads to a decrease in the growth rates of the unstable disturbances.

Recent Russian papers, (Dovgal *et al.*, 1989a,b; Fedorov *et al.*, 1991) indicate that wind tunnel experiments confirmed the stabilizing effect of localized surface heating, at least for some configurations. Fig. 6 shows experimental results obtained on a two-dimensional flat plate placed in a subsonic wind tunnel (Dovgal *et al.*, 1989a). The wall is heated from $x = 0$ to $x = 0.1$ m and the wall temperature without heating is 296 K. The figure presents the streamwise evolution of the velocity fluctuations (rms values) measured near the wall without heating and for two cases with heating ($T_w = 365$ and 381 K). The efficiency of this stabilization technique is obvious. The points on the x-axis correspond to the theoretical transition location predicted by the e^n method with the value of the n factor corresponding to the case without heating. It is interesting to observe that

the theory is able to reproduce the transition movement, at least qualitatively. Other measurements (Dovgal *et al.*, 1989a) demonstrated that the best results are obtained when the heated strip is located in the area where the TS waves start to develop. Negative results (transition moves upstream) are obtained if heating is applied too far downstream of this area, because the destabilizing effect due to the heated strip becomes more important than stabilization in the relaxation region.

As far as three-dimensional flows are concerned, the experiments reported in (Dovgal *et al.*, 1989b) show that it is very difficult to observe a positive effect of the localized heating when transition is dominated by crossflow disturbances. Computations using the e^n method supported this conclusion (see Arnal, 1996).

Linear and nonlinear, non local theory: PSE approach

A new formulation of the stability analysis was proposed by Herbert (1993). The advantages of this so-called PSE approach (Parabolized Stability Equation), is that nonparallel effects are accounted for (nonlocal theory) and that nonlinear terms can be introduced into the equations.

The use of the *linear* PSE approach for transition prediction is similar to that of the classical, local theory. In particular, it is possible to integrate the (nonlocal) growth rates in the flow direction and to apply the e^n method to predict the onset of transition. Although the disturbance growth rates from local and nonlocal theories can differ significantly, particularly for three-dimensional flows (Arnal, 1995), the basic problem for transition prediction remains the same, i.e. one has to choose a value of the n factor at transition.

The *nonlinear* PSE approach is much more interesting because it is able to model resonances between different unstable modes. This can result in a steady distortion of the basic flow which is interpreted as the onset of transition. In other words, the concept of the "critical n factor" does not exist for nonlinear PSE.

As an example of application of nonlinear PSE computations, Fig. 7 shows the effect of suction on the stability properties for a two-dimensional flow (Casalis *et al.*, 1995). The results are related to a flat plate flow with a free stream velocity of 50 m/s. Suction is applied over a streamwise extent of 10 cm with a vertical suction velocity V_w equal to -1 cm/s. The numbers between parentheses denote the beginning and the end of the suction region. The left hand part of this figure shows the evolution of the amplitude $A_{2,0}$ of the primary, two-dimensional wave. The right hand part presents the variation of the amplitude $A_{1,1}$ of the secondary, oblique mode (H-type peak-valley system). It can be seen that suction location has only a minor effect on the primary mode, but this effect becomes important for the oblique mode: if suction starts upstream of $X = 0.5$ m, the secondary mode is damped up to the end of the plate. If suction starts at $X = 0.6$ or 0.7, resonance occurs. This demonstrates that suction is efficient if it is applied in the linear growth rate regime, i.e. before the appearance of the peak-valley system. Fundamental wind tunnel experiments performed by Reynolds & Saric

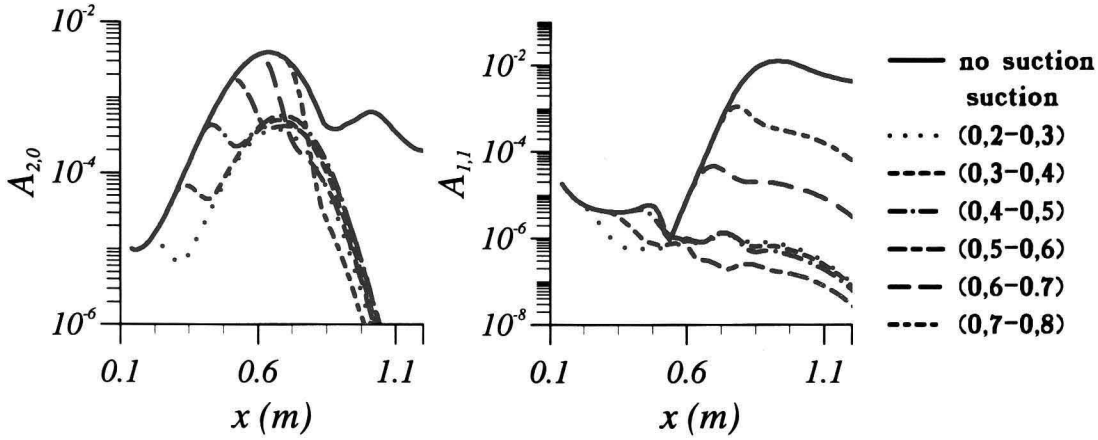

Figure 7: Effect of suction location on resonance.

(1982) indicated that suction is more effective when applied at Reynolds numbers close to the lower branch of the neutral curve, in qualitative agreement with the previous theoretical results.

"Natural" disturbances along attachment line

Even in the absence of leading edge contamination, unstable waves may appear and grow along the attachment line of swept wings. They have been observed, for instance, by Pfenninger & Bacon (1969) and by Poll (1978). This simplest way to investigate the linear problem is to use the classical, parallel theory for Tollmien-Schlichting waves (Orr-Sommerfeld equation). Based on this theory, the critical Reynolds number $\bar{R}_{cr}$ is about 670. It is also possible to follow a more rigorous approach by considering two-dimensional Görtler-Hämmerlin (GH) disturbances. In this approach, the disturbance amplitude in the X-direction normal to the leading edge depends linearly on X. The parallel flow assumption is no longer necessary, so that the GH disturbances are exact solutions of the linearized Navier- Stokes equations. The critical Reynolds number is now about 580 (see Hall *et al.*, 1984), in good agreement with the experimental data. Numerical investigations by Spalart (1988) and Lin & Malik (1995) indicated that the two-dimensional GH disturbances were the most amplified ones in the incompressible attachment line boundary layer.

Experiments on natural transition were conducted on a swept wing equipped with a suction system along the leading edge. This wing was the model without Gaster bump previously used for the investigation of leading edge contamination. The experimental set-up was modified in order to displace the apex of the model 300 mm above the wind tunnel floor, see Fig. 8. Regular waves travelling along the attachment line were detected by hot film measurements. When suction (blowing) is applied, the value of $\bar{R}$ at which the waves are observed increases (decreases) rapidly. It can be seen in Fig. 9 that the trend is in qualitative

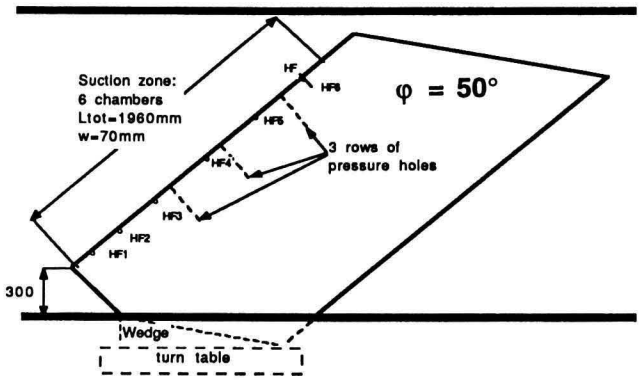

Figure 8: "Natural" transition along the attachment line of a swept model: experimental set-up.

agreement with theoretical results. In the experiments, the maximum value of $\bar{R}$ (close to 800) is fixed by the maximum wind tunnel speed.

An attempt was made to use the e_n method to predict the onset of transition along the attachment line. Fig. 10 shows the spanwise evolution of the integrated growth rates in a case with $\bar{R} \approx 740$ and $K = 0$. $Z = 0$ corresponds to the apex (stagnation point) of the model where the attachment line boundary layer starts to develop. The pressure distribution around the model was first determined by inviscid computations taking into account the presence of the wind tunnel walls. In a second step, accurate boundary layer computations along the leading edge were performed by using a three-dimensional boundary layer code (Malecki *et al.*, 1993). Then two n factors were computed, one for TS waves, the second for GH disturbances. As the boundary layer results indicate that the infinite swept wing conditions are approximately reached at $Z \approx 0.25$ m, the unstable waves leading to transition do not start to develop upstream of this point. However, if the attachment line boundary layer is assumed to be uniform all along the leading edge, i.e. if is immediately equal to 740 at the apex, then GH disturbances start to be amplified at $Z = 0$ and the n factor curve is represented by the dotted line plotted in Fig. 10. Experimentally, transition was found to occur at $Z \approx 0.6$ m. This leads to the following remarks

- when the infinite swept wing assumption is used for the GH disturbances, the n factor at transition is close to 10, in agreement with previous investigations based on the same assumptions (Arnal, 1993; Lin & Malik, 1995);
- the n factor of the GH disturbances is reduced to about 3 to 4 when the upstream flow history is taken into account;
- the n factor of the TS waves is close to zero.

In any case, a fundamental problem remains: the frequency range of the observed unstable waves is lower than that predicted by the theory (around 6 kHz

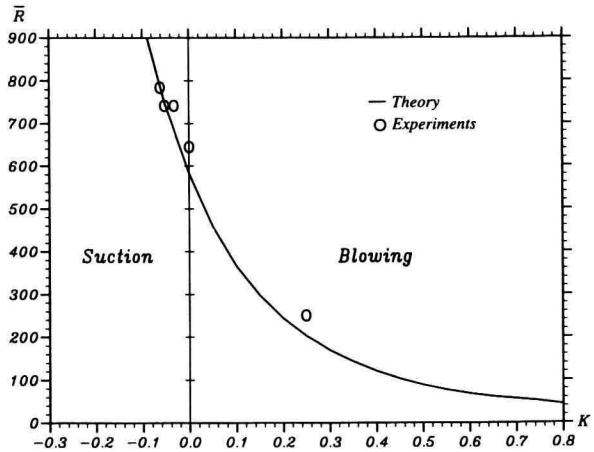

Figure 9: Suction effect on "natural" transition Reynolds number along the attachment line.

in the experiments, around 7 kHz in the computations). In fact, the measured frequency range is close to the lower branch of the neutral GH disturbances, as observed in previous experiments (Poll, 1978; Pfenninger & Bacon, 1969). This discrepancy could be explained by nonlinear phenomena which are not yet fully understood (Hall & Malik, 1986; Theofilis, 1994).

Conclusion

For the purpose of skin friction drag reduction by laminar flow control, it is often necessary to delay the onset of leading edge contamination. This can be done either by using a Gaster bump or by applying suction along the attachment line. For a given aircraft, the choice of the most appropriate device depends on the value of $\bar{R}$ near the root (leading edge radius, sweep angle, cruise conditions) and also on technological possibilities (for instance the use of anti-icing systems can make suction systems difficult to handle). Numerical and experimental investigations provided some interesting insight into the capabilities and limitations of such devices.

As far as natural transition is concerned, the e^n method remains a very efficient tool for parametric studies. Of course, there are so many routes to turbulence that a "universal" value of n cannot exist. This is true for the "old", local method, but also for the "new", nonlocal method based on linear PSE. The major improvement of nonlinear PSE is that transition occurs naturally, because resonance mechanisms are now included in the model. The new problem is the choice of correct initial conditions (amplitude, frequency, orientation) which are unknown for most of the real flow situations.

The attachment line instability is a particular problem which is likely to be important for large transport aircraft as soon as leading edge contamination is

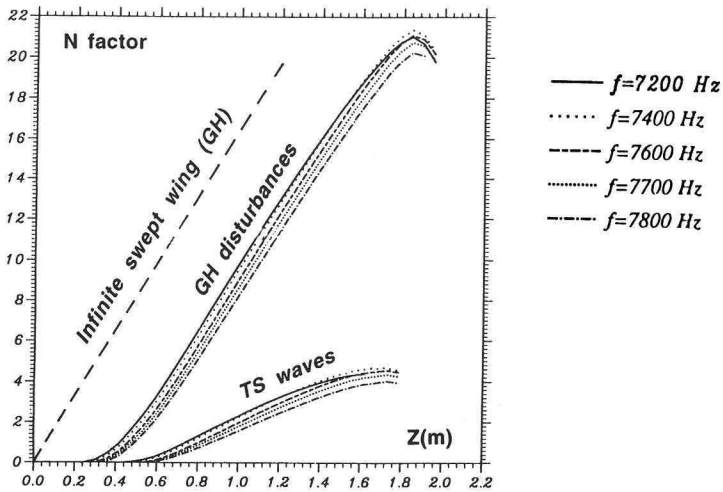

Figure 10: N factors for TS and GH disturbances.

avoided. It is now clear that GH disturbances play a major role; the present experiments showed that they can be damped by suction levels which are much lower than those necessary to relaminarize a contaminated turbulent boundary layer. However several problems still need to be solved, in particular those associated with nonlinear (subcritical ?) phenomena and with the use of the e^n method.

References

AGARD Report 786, 1992 – Special Course on Skin Friction Drag Reduction.

Arnal, D. 1993 – Prediction based on linear theory. In Progress in Transition Modelling, AGARD Report 793.

Arnal, D., Casalis G. & Juillen J.C. 1995 – A survey of the transition prediction methods: from analytical criteria to PSE and DNS. In R. Kobayashi, Editor, Laminar-Turbulent Transition, IUTAM Symp., Sendai, Springer Verlag.

Arnal, D., 1996 – Etude numérique de l'effet d'un chauffage localisé sur la transition. To be published.

Casalis, G., Copie, M.L., Airiau, C. & Arnal, D. 1995 – Nonlinear analysis with PSE approach. IUTAM Symposium on Nonlinear Instability and Transition in Three-dimensional Boundary Layers, Manchester.

Dovgal, A.V., Levchenko, V.Ya. & Timofeyev, V.A. 1989a – Laminarisation of the boundary layer through localised surface heating. In Proceedings of the Siberian Section of the USSR Academy of Sciences, Novosibirsk.

Dovgal, A.V., Levchenko, V.Ya. & Timofeyev, V.A. 1989b – Action of local heating on the transition to turbulence in a three-dimensional gas boundary layer. In Proceedings of the Siberian Section of the USSR Academy of Sciences, Novosibirsk.

Fedorov, A.V., Levchenko, V.Ya. & Tumin, A.M. 1991 – Problems of laminar-turbulent transition control in a boundary layer. *Russian J. of Theoretical and Applied Mechanics* **1**, 85-101.

Gaster, M., 1967 – On the flow along leading edges. *Aeron. Quart.* **18**.

Hall, P., Malik, M.R. & Poll, D.I.A. 1984 – On the stability of an infinite swept attachment line boundary layer. *Proc. R. Soc. London A* **395**, 229-245.

Herbert T., 1993 – Parabolized stability equations. In Progress in Transition Modelling, AGARD-FDP-VKI Special Course.

Juillen, J.C. & Arnal, D. 1995 – Experimental study of boundary layer suction effects on leading edge contamination along the attachment line of a swept wing. In R. Kobayashi, Editor, Laminar-Turbulent Transition, IUTAM Symp., Sendai, Springer Verlag.

Lin, R.S. & Malik, M.R. 1995 – The incompressible attachment line boundary layer stability. In R. Kobayashi, Editor, Laminar-Turbulent Transition, IUTAM Symp., Sendai, Springer Verlag.

Malecki, P., Cousteix J. & Houdeville, R. 1993 – Three-dimensional boundary layer calculations with two-layer turbulence models. 5th Int. Symp. on Refined Flow Modelling and Turbulence Measurements, Paris.

Pfenninger, W. 1965 – Flow phenomena at the leading edge of swept wings. AGARDograph 97, Part 4.

Pfeninnger, W. & Bacon Jr., J.W. 1969 – Amplified laminar boundary layer oscillations and transition at the front attachment line of a 45 swept flat-nosed wing with and without boundary layer suction. Viscous Drag Reduction, C.S. Wells Ed., Plenum Press.

Poll, D.I.A. 1978 – Some aspects of the flow near a swept attachment line with particular reference to boundary layer transition. Technical Report 7805./K, Cranfield, College of Aeronautics.

Poll, D.I.A. & Danks, M. 1995 – Relaminarisation of the swept wing attachment line by surface suction. In R. Kobayashi, Editor, Laminar-Turbulent Transition, IUTAM Symp., Sendai, Springer Verlag.

Reynolds, W.S. & Saric, W.S. 1982 – Experiments on the stability of the flat plate boundary layer with suction. AIAA Paper 82-1026.

Spalart, P.R. 1988 – Direct numerical study of leading edge contamination. AGARD CP 438.

Theofilis, V. 1994 – On subcritical instability of the attachment line boundary layer. AGARD CP 551.

Authors' addresses

°CERT ONERA – DERAT
2 avenue E. Belin
F–31055 Toulouse Cedex, France

▹ONERA – OA
B.P. 72
92322 Chatillon Cedex, France